International Journal of Applied Research 2019; 5(1): 440-443

ISSN Print: 2394-7500
ISSN Online: 2394-5869
Impact Factor: 5.2
IJAR 2019; 5(1): 440-443
www.allresearchjournal.com
Received: 16-11-2018
Accepted: 19-12-2018

Anshu Kumari
Former, Research Scholar, Department of Physics, LNMU, Darbhanga, Bihar, India

Corresponding Author:
Anshu Kumari
Former, Research Scholar, Department of Physics, LNMU, Darbhanga, Bihar, India

Studies the optical properties of multi-coupled silver nanoshell particles

Anshu Kumari

Abstract
The shift of the nanoshell plasmon resonances wavelength is plotted against with different dielectric environments, several different dielectric cores, the ratio of the inner and outer radius, and also its assemblies. The results show that a red- and blue-shifted localized surface plasmon can be tuned over an extended wavelength range by varying dielectric environments, the dielectric constants and the radius of nanoshell core respectively. In addition, the separation distances, the distribution of electrical field intensity, the incident directions and its polarizations are also investigated. The study is useful to broaden the application scopes of Raman spectroscopy and nano-optics.

Keywords: Optical Properties, Silver and Nanoshell

Introduction
Plasmon resonances are electromagnetic modes associated with the excitation of collective oscillations of the electronic charge density in metals. When plasmon is under certain electromagnetic disturbance, according to metallic electrical theory, charge density may not be zero in some regions, and a restoring force will be generated to induce oscillating charge distribution. When frequencies of the electromagnetic disturbance and the plasmon oscillation match each other, resonance will happen. The oscillation frequency is determined by four factors: the density of electrons, the electron mass, the size and the shape of the charge distribution. The metal surface plasmon resonances is the main factor in determining the optical properties of metal nanoparticles. Many unique optical properties can be achieved when adjusting the structure, morphology, size, nanoshell and composition of the metal nanoparticles [1-9]. Consequently, manufacturing and application of metallic nanoparticles have become very active topics in materials science.
Furthermore, the strong optical field generated in these systems could be used in surface enhancement Raman scattering [10, 11], devise new configuration for chemical and material science [12, 13]. As all these devices are strongly sensitive to the light frequency, it could be interesting to dispose tunable nanoparticles to modify their frequency range.

Numerically analysis
There are some numerical simulation methods to study the interaction between the light and metal spheres such as FDTD (Finite-difference Time-domain), FEM (Finite Element Method), DDA (Discrete-dipole Approximation) and Green's function or called CDA (Coupled-dipole Approximation). In this paper, Green's function is used to study the optical properties of silver nanoshell particles. First, let's briefly outline the main features of the theoretical scattering formalism with the Green's function on which the numerical simulation is based and associated numerical method. Given a scattering object with a dielectric function $\varepsilon_s(\mathbf{r}, \omega)$ embedded in an infinitely homogenous background medium with a dielectric parameter of $\varepsilon_m(\mathbf{r}, \omega)$, we can assume that the electric and magnetic fields have a harmonic time dependence $\exp(-i\omega t)$ in Maxwell's equations. When this system is illuminated by an incident field in the background medium, the vectorial wave equation for electric field can be expressed as:

$$\nabla \times \nabla \times \boldsymbol{E}(\boldsymbol{r}, \omega) - k_0^2 \varepsilon_m(\boldsymbol{r}, \omega) \boldsymbol{E}(\boldsymbol{r}, \omega) = k_0^2 [\varepsilon_s(\boldsymbol{r}, \omega) - \varepsilon_m(\boldsymbol{r}, \omega)] \boldsymbol{E}(\boldsymbol{r}, \omega) \quad (1)$$

Where ε_s and ε_m are the scattering dielectric constant and system dielectric constant respectively, and $k0$ is the wave number in vacuum.

The method of solving scattering field is based on the Lippmann-Schwinger equation $\mathbf{E} = \mathbf{E}_{inc} + \mathbf{E}_s$, where $\mathbf{E}_{inc}$ and $\mathbf{E}s$ are the incident field and the scattering field respectively. Taking the Dirac delta function into account, Eq. 1 can be resolved to the following three-dimension vector Lippmann-Schwinger integral equation:

$$\boldsymbol{E}(\boldsymbol{r},\omega) = \boldsymbol{E}_{inc}(\boldsymbol{r},\omega) + \int_{V_d} \boldsymbol{G}_0(\boldsymbol{r},\boldsymbol{r}',\omega)\Delta\varepsilon(\boldsymbol{r}',\omega)\boldsymbol{E}(\boldsymbol{r}',\omega)d^3\boldsymbol{r}' \quad (2)$$

$\mathbf{G}_0(\mathbf{r}, \mathbf{r}', \omega)$ is the Green's tensor for an infinitely homogeneous background medium ε_m, which is expressed as:

$$\boldsymbol{G}_0(\boldsymbol{r},\boldsymbol{r}',\omega) = k_0^2\left(\boldsymbol{I} + \frac{ik_mR-1}{k_m^2R^2}\boldsymbol{I} + \frac{3-3ik_mR-k_m^2R^2}{k_m^2R^4}\boldsymbol{RR}\right) \times \frac{\exp(ik_mR)}{4\pi R}, \qquad \boldsymbol{r}\neq\boldsymbol{r}', \quad (3)$$

Where $\mathbf{I}$ is the unit dyadic, $\mathbf{R} = \mathbf{r} - \mathbf{r}'$, $R = |\mathbf{r} - \mathbf{r}'|$ and $¦\varepsilon(\mathbf{r}', \omega) = \varepsilon_s - \varepsilon_m$. There is a singularity in Eq. 2 when $\mathbf{r} = \mathbf{r}'$, which have been solved by Yaghjian in detail [14]. The implicit Eq. 2 can be solved via numerical simulation based on discretization, which results in:

$$\boldsymbol{E}(\boldsymbol{r}_i,\omega) = \boldsymbol{E}_{inc}(\boldsymbol{r}_i,\omega) + \sum_{j=1}^{N}\boldsymbol{G}(\boldsymbol{r}_i,\boldsymbol{r}_j,\omega)\Delta\varepsilon_j\boldsymbol{E}(\boldsymbol{r}_j,\omega)V_j, \quad i=1,\cdots,N \quad (4)$$

V_j is the volume of the scattering particle. Since the scalar Green's tensor is dependent only on the absolute relative distance $\mathbf{R}$, and is reciprocal, i.e., $\mathbf{G}(\mathbf{r}_i, \mathbf{r}_j) = \mathbf{G}(\mathbf{r}_j, \mathbf{r}_i)$, or written as $\mathbf{G}(\mathbf{r}_i, \mathbf{r}_j) = \mathbf{G}_{i-j}$. We can generate the following equation by substituting $\mathbf{G}(\mathbf{r}_i, \mathbf{r}_j) = \mathbf{G}_{i-j}$ into Eq. 4 and rearranging terms:

$$\sum_{j=1}^{N}\left(\boldsymbol{I} - \boldsymbol{G}_{i-j}\Delta\varepsilon_jV_j\right)\boldsymbol{E}_j = \boldsymbol{E}_{inc}(\boldsymbol{r}_i,\omega), \qquad i=1,\cdots,N \quad (5)$$

$\mathbf{E}_j$ and $\mathbf{E}_{inc}$ are 3N-dimensional vector, while $\mathbf{G}_{i-j}$ is a 3N × 3N matrix. The total electric field can be derived, along with spectral and optical parameters, after solving these 3N complex linear equations. The researchers could obtain magnetic field $\mathbf{H}$ and Poynting vector $\mathbf{S}$ with the similar method. The optical efficiencies (i.e., extinction cross section, absorption cross section and scattering cross section) are defined as:

$$C_{ext} = \frac{4\pi k}{|\boldsymbol{E}_{inc}|^2}\sum_{i=1}^{N} Im\left(\boldsymbol{E}_{inc,i}^{*}\cdot\boldsymbol{P}_i\right),$$
$$C_{abs} = \frac{4\pi k}{|\boldsymbol{E}_{inc}|^2}\sum_{i=1}^{N}\left\{Im\left[\boldsymbol{P}_i\cdot\left(\alpha_i^{-1}\right)^{*}\boldsymbol{P}_i^{*}\right] - \frac{2}{3}k^3|\boldsymbol{P}_i|^2\right\} \quad (6)$$

Where * means complex conjugate,

$\mathbf{P}_i = \alpha_i \cdot \mathbf{E}_{loc}$, $\mathbf{E}_{loc} = [(\varepsilon_s + 2\varepsilon_m)/3]\mathbf{E}$

with $\frac{(\varepsilon_s(r_i,\omega)-\varepsilon_m(r_i,\omega))}{(\varepsilon_s(r_i,\omega)+2\varepsilon_m(r_i,\omega))}\frac{3V}{4\pi}$, and scattering cross section can be obtained by $C_{sca} = C_{ext} - C_{abs}$. The extinction and absorption efficiency are $Q_{ext} = C_{ext}/S$ and $Q_{sca} = C_{sca}/S$ respectively, S is the effective area of scattering particles.

Results and Discussion

In this paper, the optical properties of silver nanoshell particles are studied, the numerical simulation system is given in Fig. 1. The optical constants for silver are taken from reference [15]. Spectroscopic effects occur when the dielectric response of the particles shows a strong dispersion as a function of the incident wavelength. It is well known that the dielectric response of metals displays this behavior which is associated with the phenomenon of local plasmon resonances of small metallic particles for the variation wavelengths. The physical and chemical properties of metallic nanoshell have been studied in recent years due to their attractive features which make them used in nanoscale optical regions.

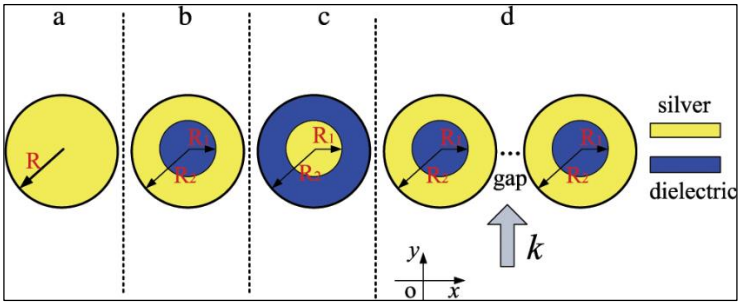

Fig 1: Numerical simulation system, where yellow one denotes silver, while blue one is dielectric, R is radius (R_1 and R_2 are inner and outer radius) and gap denotes separation gap, *K* is incident wave propagate direction. a, b, c and d denote a solid silver sphere, a dielectric core-silver shell, a silver core-dielectric shell and two interacted silver nano-shell spheres respectively

Firstly, to get resonance behaviors, the influences of the mediums surrounding to the extinction efficiency of a solid silver sphere are studied with radius 25 nm (see Fig. 1 case of a, R = 25 nm) as a function of the incident wavelength by plane wave. Spectroscopes are given with infinite homogeneous medium in vacuum (n = 1.00), water (n = 1.33) and SiO_2 (n = 1.50) respectively. We can see an increase intensity which is materialized by a peak in its variation with the incident wavelength at about λ = 370 nm in vacuum, λ = 400 nm in water and λ = 410 nm in SiO_2.

Silver-core SiO_2-shell nanoparticles have been used for probing spatial distribution of electrical field enhancement

via surface-enhanced Raman scattering. In addition, the SiO_2 core-silver shell with different inner radius are also reported with the outer radius 25 nm, seen in Fig. 2.

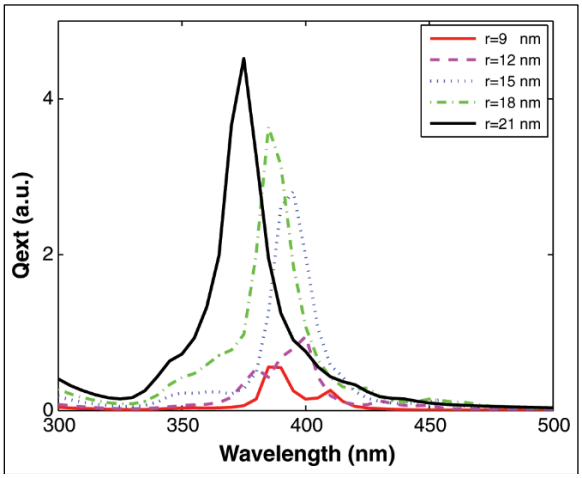

Fig 2: The extinction efficiency of SiO_2 core-silver shell for different inner radius values from 9 nm to 21 nm with outer radius 25 nm

It shows that the peak's position is blue-shifted with increasing inner radius, and there is a second smaller peak when radius is smaller, while only one single peak for bigger radius and the intensity seems to enhance straightly. It is worth noting that the plasmon resonance is quiet sensitive to the thickness of silver shell and dielectric core. It means that the plasmon resonance peak's position also could be tuned over an extended wavelength by varying the ratio of the inner and outer radius.

$$\varepsilon_c = -2\varepsilon_s \frac{\varepsilon_s(1-f)+\varepsilon_m(2+f)}{\varepsilon_s(1+2f)+2\varepsilon_m(1-f)} \qquad (7)$$

Where ε_c, ε_s and ε_m are the dielectric constants of the core, shell, and medium, respectively, and f is the fraction of the volume of the core in the composite structure. It is interesting to note that f is essentially (t/R + 1) −3, where t is the nanoshell thickness and R is the core radius. In other words, a larger core has a larger polarizability and a thin shell gets stronger near-field coupling, thus leading to a larger fractional plasmon shift. This analogy serves to qualitatively explain the similarity of the distance dependence and scaling behavior of plasmon coupling in the nanoshell structure to that in the particle-pair structure. The cores in the nanoparticles can be considered as truncated waveguide; the core or cavity between the nanoshell is open to the free space and forms a low-Q-cavity resonator.

Thirdly, the coupling silver nanoshell spheres are also studied. A solid silver sphere has only one plasmon resonance due to its symmetry, but new resonances may appear when they are collected in assemblies, which are depend on the symmetry of its assemblies. Figure 3 shows the extinction efficiency for SiO_2 core-silver shell spheres collected by small coupling spheres with two, three, and four nanoparticles in vacuum (n = 1.00) illuminated by plane wave with polarization parallel to the inter-spheres. The parameters of silver nanoshell sphere are the same as the above mode, with a SiO_2 core of inner radius R_1 = 15 nm and an outer radius R_2 = 25 nm, thus a silver shell of thickness 10 nm. Two, three and four silver nanoshell spheres are touched but not interpenetrated, seen in the top of Fig. 3.

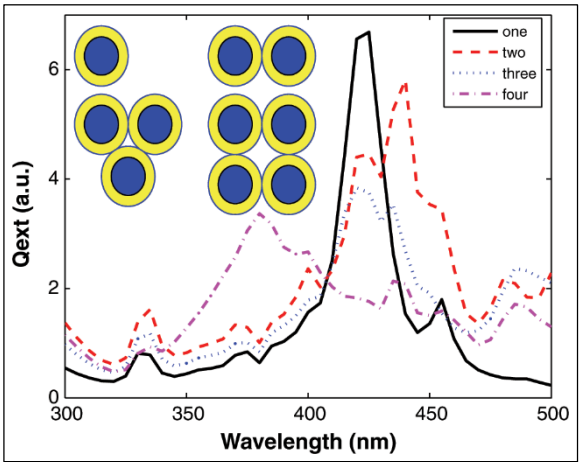

Fig 3: The extinction efficiency of SiO_2 core-silver shell with one, two, three, and four nano-shell silver spheres

It can be observed that there are new resonance modes and are red-shifted with increasing the number of silver nanoshell spheres from 2 to 4 compared with one single solid silver sphere. And the position of plasmon resonance peak are new red-shifted bands and there are more small peaks due to adding more sharp corners or singularities for touching interfaces with more spheres, which play an important role to scattering intensity.

The red-shifted plasmon excitation has been enhanced by the dielectric core or silver core nanoshell through a "waveguide effect". And then, the role plays of the separation distances between silver nanoshell and nanoshell sphere pairs are also studied. Figure 4 shows the spectra of extinction efficiency for a single silver nanoshell sphere and nanoshell sphere pairs with radius 50 nmof different gap distances from 0 to 20 nm as a function of wavelengths with polarization parallel to intersphere.

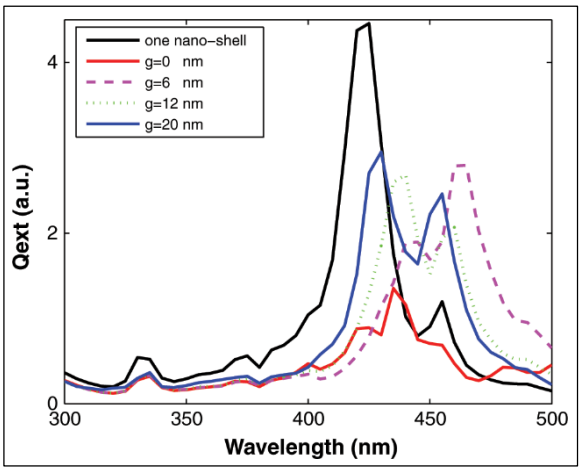

Fig 4: The extinction efficiency of line chains of two SiO_2 coresilver shell with different separation gaps from g = 0 nm to g = 21 nm

It shows that when the gap distance g increases, the peak's position of extinction efficiency shows red-shifted for very smaller g firstly, while blue-shifted for larger g in visible light region, and the intensity enhanced firstly and then decreases as the gap distance larger. In addition, the silver nanoshell spheres with the ration of different distance gap and radius are considered (the radius/gap ratio remains

constant), silver nanoshell sphere pairs radius varied from 20 to 50 nm as a function of wavelengths. It shows that the peak's position of extinction efficiency shows red-shifted with distance gap and radius increasing in visible light region (the result is not given here). The new plasmon modes are likely due to oscillations along the intersphere axis or interface plane. It is also found that the peak's position is red-shifted with increasing the numbers of silver nanoshell spheres in a linear chains of two, three, four and more SiO_2 coresilver shell particles.

Conclusions

The unique properties of this nanostructure are highly attractive for serving as resonant nanocavities to hold and probe smaller nanostructures, such as quantum dots. Due to their strong and tunable plasmon resonance, nanoshells may be useful applications in nano-optical devices, surface-enhanced Raman spectroscopy, chemical and biological sensors.

Furthermore, the strong frequency sensitivity of these coupled resonances could be used to produce frequency-selective devices in the future.

References

1. Kelly KL, Coronado E, Zhao LL, Schatz GC. The optical properties of metal nanoparticles: the influence of size, shape, and dielectric environment. J Phys Chem B 2003;107:668.
2. Zhang Q, Tan YN, Xie J, Lee JY. Colloidal synthesis of plasmonic metallic nanoparticles. Plasmonics 2009;4:9.
3. Sun Y, Xia Y. Shape-controlled synthesis of gold and silver nanoparticles. Science 2002;298:2176.
4. Nehl CL, Liao H, Hafner JH. Optical properties of star-shaped gold nanoparticles. Nano Lett 2006;6:683.
5. Talley CE, Jackson JB, Oubre C, Grady NK, Hollars CW, Lane SM, Huser TR, Nordlander P, Halas NJ. Surface enhanced Raman scattering from individual Au nanoparticles and nanoparticle dimer substrates. Nano Lett 2005;5:1569.
6. Zhang ZY, Zhao YP. Optical properties of helical Ag nanostructures calculated by discrete dipole approximation method. Appl Phys Lett 2007;90:221501.
7. Wu DJ, Xu XD, Liu XJ. Tunable near-infrared optical properties of three-layered metal nanoshells. J Chem Phys 2008;129:074711.
8. Hoflich K, Gosele U, Christiansen S. Near-field investigations of nanoshell cylinder dimmers. J Chem Phys 2009;131:164704.
9. Kottmann JP, Martin OJF. Field polarization and polarization charge distributions in plasmon resonant nanoparticles. New J Phys 2000;2:271.
10. Maier SA. Plasmonics: fundamentals and application. Springer 2007.
11. Novotny L, Hecht B. Principles of nano-optics. Cambridge University Press, Cambridge 2006.
12. Prodan E, Radloff C, Halas NJ, Nordlander P. A hybridization model for the plasmon response of complex nanostructures. Science 2003;302:419.
13. Haes AJ, Zou S, Schatz GC, Van Duyne RP. Nanoscale optical biosensor: short range distance dependence of the localized surface plasmon resonance of noble metal nanoparticles. J Phys Chem B 2004;108:6961.
14. Yaghjian AD. Electric dyadic Green's functions in the source region. Proc IEEE 1980;68:248.
15. Johnson PB, Christy RW. Optical constants of the noble metals. Phys Rev B 1972;12:4370.